https://doi.org/10.3311/PPci.19996



**Periodica Polytechnica Civil Engineering**, 66(4), pp. 1087–1097, 2022

# Road Pavement Asphalt Concretes for Thin Wearing Layers: A Machine Learning Approach towards Stiffness Modulus and Volumetric Properties Prediction

Nicola Baldo[1*], Matteo Miani[1], Fabio Rondinella[1], Evangelos Manthos[2], Jan Valentin[3]

[1] Polytechnic Department of Engineering and Architecture (DPIA), University of Udine, Via del Cotonificio 114, 33100 Udine, Italy
[2] Department of Civil Engineering, Aristotle University of Thessaloniki, University Campus, 54124 Thessaloniki, Greece
[3] Faculty of Civil Engineering, Czech Technical University, Thákurova 7, 166 29 Prague, Czech Republic
[*] Corresponding author, e-mail: nicola.baldo@uniud.it

Received: 09 February 2022, Accepted: 11 July 2022, Published online: 15 July 2022

**Abstract**

In this study a novel procedure is presented for an efficient development of predictive models of road pavement asphalt concretes mechanical characteristics and volumetric properties, using shallow artificial neural networks. The problems of properly assessing the actual generalization feature of a model and avoiding the effects induced by a fixed training-test data split are addressed. Since machine learning models require a careful definition of the network hyperparameters, a Bayesian approach is presented to set the optimal model configuration. The case study covered a set of 92 asphalt concrete specimens for thin wearing layers.

**Keywords**

thin surface layer, mix design, stiffness modulus, machine learning, Bayesian optimization

## 1 Introduction

A well-designed road pavement, both in terms of layers' size and material's response under the traffic and climate loads, is crucial to ensure adequate levels of service and safety to road users. The first step to avoid the most common failure modes, such as fatigue or low-temperature cracking, permanent deformation and stripping, is to design the mix by means of a performance optimization process based on mechanical and volumetric behavior models of asphalt concrete (AC) [1]. These models define the response of the material with respect to its composition. However, the approach currently used by the road engineer involves performing experimental tests to evaluate the response of the asphalt concrete made in the laboratory, with a specific bitumen content and a defined aggregate gradation [2]. Therefore, any change to the composition of this mixture, even during on-site production, requires new costly laboratory tests. In recent years, the search for a mathematical or numerical model that can reliably predict the asphalt mix response has been the focus of many researchers in the field of road pavement engineering. Two main approaches may be implemented for this purpose: advanced constitutive modeling or soft computing techniques. The former consists in using fundamental and rational constitutive laws of the mechanics [3]. The latter, which has been shown to produce more accurate predictions than statistical regressions [4], exploits forecasting artificial neural networks (ANNs). ANNs are nonlinear fitting systems that mimic the biological learning process to correlate experimental data. A detailed description of the mathematical framework can be found in the relevant literature. ANNs have been applied to evaluate the characteristics and performance of asphalt pavements with the aim of introducing novel approaches to an empirical-mechanical mix design. Ozsahin and Oruc [5] employed a three-layer feed-forward neural network to determine the relationship between the resilient modulus of emulsified asphalt mixture and some predictors (such as curing time, cement addition level, and residual asphalt content), demonstrating that artificial intelligence is an excellent method to reduce the time consumed at the design stage. Tapkın et al. [6] presented an application of ANN to model the creep behavior under repeated loading of polypropylene modified asphalt concretes. Conversely, Mirzahosseini et al. [7] have studied the rutting potential of dense asphalt concretes, implementing a multilayer perceptron ANN that maps the pattern between the flow number and some features of standard Marshall specimens, such as

**Cite this article as:** Baldo, N., Miani, M., Rondinella, F., Manthos, E., Valentin, J. "Road Pavement Asphalt Concretes for Thin Wearing Layers: A Machine Learning Approach towards Stiffness Modulus and Volumetric Properties Prediction", Periodica Polytechnica Civil Engineering, 66(4), pp. 1087–1097, 2022. https://doi.org/10.3311/PPci.19996

the aggregate and bitumen contents, percentage of voids in mineral aggregate and Marshall test results. Accurate predictions of the fatigue performance [8, 9] and the dynamic modulus [10] of hot mix asphalt under various loading and environmental conditions were also produced by means of the artificial intelligence. As the mechanical characteristics of asphalt concrete also depend on the volumetric properties which have to meet the limits set by local specifications, Zavrtanik et al. [11] had recourse to ANNs for modeling air void content in several aggregate mixtures. Notwithstanding the excellent results reported in the documented literature, effective procedures have not been defined for tuning the model settings, called hyperparameters, and then for the identification of the ANN structure (also called optimal NN model) matching the best score on predicting performance. In fact, the model hyperparameters, such as the number of neurons in the hidden layers or iterations of the training algorithm, define the network architecture, the algorithmic functioning and consequently the model predictive skills. Optimal ANN settings are commonly defined by means of a trial-and-error procedure [7, 12], such as grid or random search, but the evaluation of the performance function score for different hyperparameters is extremely expensive, in terms of time-consuming [13]. In this context, Bayesian Optimization offers an efficient and semi-autonomous process for fine-tuning the hyperparameters of the optimal NN model [14]. By keeping a record of past evaluations, the Bayesian approach builds a probabilistic model of the performance function, which is used to make decisions on the next set of hyperparameters to be evaluated so that the expected error is minimized [15, 16]. The aim of this study was to implement and apply an unbiased procedure for the optimal ANN model selection, using Bayesian processes, of a given predictive modeling problem. In particular, the case study involved a set of 92 variants of road pavement asphalt concretes for thin wearing layers, prepared in the laboratory or in plant with different binder types, bitumen contents and aggregate gradations. The ANN approach was used to identify a reliable correlation of the stiffness modulus (IT-CY), air voids (AV) and voids in the mineral aggregate (VMA) to the main mix composition variables, such as bitumen content (% by weight of mix), percentages of aggregate passing at 6.3 mm and 0.063 mm sieves.

## 2 Materials and experimental design

The type of HMA mixture considered in the current study was a semi-open graded asphalt concrete for surface courses, which belongs to the broader group of asphalt concretes for very thin layers (AC-VTL) as described in EN 13108-2 [17]. Asphalt Concrete for Very Thin (surfacing) Layer was originally developed in France during the '80s, called Bétons bitumineux très minces (BBTM). The original idea was to produce an asphalt mixture for surface course that would separate the role of the wearing course from the rest asphalt layers and which would be laid at a thickness of 20 mm to 30 mm. Due to its advantages over dense asphalt concrete for surface courses and other surface course mixes, AC-VTL is presently used by many countries worldwide. The main advantages of AC-VTL can be summarized to the following: a) due to its low thickness requiring lesser amount of materials, hence lowers the total cost and minimizes the quantities of hard and durable aggregates coming from natural non-renewable resource; b) due to its gap-graded gradation provides a pavement surface with very good surface characteristics, such as very good macrotexture and (with the use of hard and durable aggregates) very good skid resistance; c) provides a noise reducing surface (reduction -3 dB to -4 dB in comparison to conventional dense asphalt concrete surface); d) provides a pavement surface with a certain drainage ability, hence reduction of water spray; e) faster construction can be achieved; f) it can be used as an overlay without milling the underlying layer and not raise the surface level too much; g) up to a certain point it can improve the evenness of the pavement surface, so a levelling course not to be needed; h) in case of maintenance/renewal of the AC-VTL smaller quantities of materials are wasted or used for recycling; i) no modifications are required by the conventional mixing plants in order to produce AC-VTL. AC-VTLs for the current study were produced with diabase aggregates and two types of bitumen: conventional or modified bitumen. The production of some of the AC-VTLs was carried out in the laboratory either as part of the mix design procedure or as part of stiffness testing of the design mixture. The rest of the AC-VTLs were produced into a stationary asphalt plant as final mixture production. The aggregates used in the mixtures of the current study were diabase aggregates coming from three different quarries; the aggregates characteristic properties, as well as the test protocols used for their determination, are given in Table 1 [18–22].

As mentioned above, two types of bitumen have been used in the current study, a 50/70 conventional bitumen and an SBS modified bitumen. The characteristic properties of the two bitumen types, along with the test protocols adopted for their determination, are reported in Table 2 [23–26].

**Table 1** Diabase aggregates characteristic properties

| Property | Value |
|---|---|
| Los Angeles coefficient (%), EN 1097-2 [18] | 25 |
| Polished Stone Value (%), EN 1097-8 [19] | 55 to 60 |
| Flakiness Index (%), EN 933-3 [20] | <25 |
| Sand equivalent (%), EN 933-8 [21] | >55 |
| Methylene blue value (mg/g), EN 933-9 [22] | <10 (range of values 6.7 to 8.3) |

**Table 2** Bitumen characteristic properties

| Property | Bitumen type | |
|---|---|---|
| | 50/70 | SBS modified |
| Penetration (0.1 x mm), EN 1426 [23] | 64 | 45 |
| Softening point (°C), EN 1427 [24] | 45.6 | 78.8 |
| Elastic recovery (%), EN 13398 [25] | - | 97.5 |
| Fraas breaking point (°C), EN 12593 [26] | -7.0 | -15.0 |
| After aging | | |
| Retained penetration | - | 84 |
| Difference in softening point (°C) | - | -2.4 |

The AC-VTLs used in the current study had a maximum aggregate size of 10 mm (AC-10) in all cases. The production of mixes was made either in the laboratory or at a stationary mixing plant. The specimens of all mixes were compacted in the laboratory using an impact compactor (EN 12697-30) [27]: thirty (30) specimens with 50/70 conventional paving grade bitumen (AC-10-5070L) and thirty (30) specimens with SBS modified bitumen (AC-10-SBSL) were compacted from the mixes produced in the laboratory, while thirty-two (32) specimens with SBS modified bitumen (AC-10-SBSP) were compacted from the mixes produced in the stationary mixing plant. All mixtures, gradations and data used in the current study came from projects in Greece.

The gradations of the AC-10-5070L, AC-10-SBSL and AC-10-SBSP are given in Fig. 1. Table 5 in Appendix A shows specimens' bitumen content, respective volumetric properties (EN 12697-8) [28], and Stiffness Modulus results. Additionally, since the AC-10 of the current study is a gap graded mixture, percentages passing at sieves of 10, 6.3, 2, 0.5 and 0.063 mm have also been included in Table 5. The volumetric properties of an asphalt concrete are defined by the binder's percentage to the weight of the mix, the coarse-aggregates' gradation curve and mineral type, as well as the filler content/type and the preparation process of the mixture itself. It is important that such volumetric features have their value within well-defined ranges, set by the EU standards or local specifications, in order to ensure a resistance, stiffness and long-term durability suitable for the road pavement of interest. The percentages of AV and VMA have been determined, according to the relevant standard (EN 12697-8) [28], for both laboratory- and plant-produced mixtures. The results are shown in Table 5 for all mixtures tested. The Stiffness Modulus has been determined, for all specimens, in accordance with EN 12697-26 [29], Annex C (IT-CY, Fig. 2), assuming the following testing conditions: temperature of 20 °C, target deformation fixed at 5 μm and rise-time equal to 124 ms. The number of specimens tested for stiffness was ninety-two (92). The Stiffness Modulus results are presented in Table 5 for all mixtures tested.

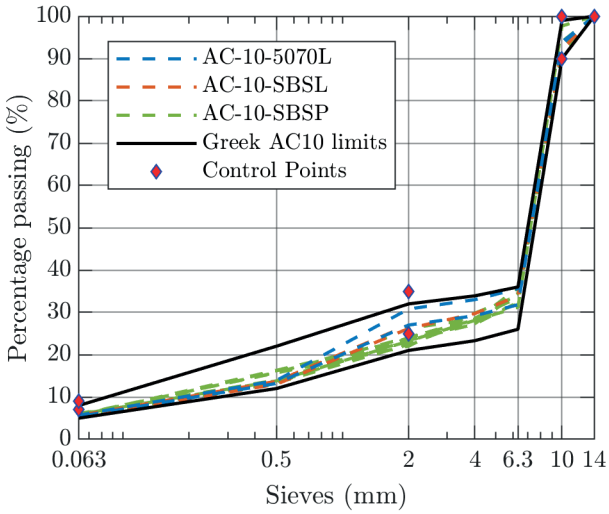


**Fig. 1** Gradation curves of AC-10-5070L (blue), AC-10-SBSL (orange), AC-10-SBSP (green) and Control Points according to EN 13108-2 [17] (BBTM10A)

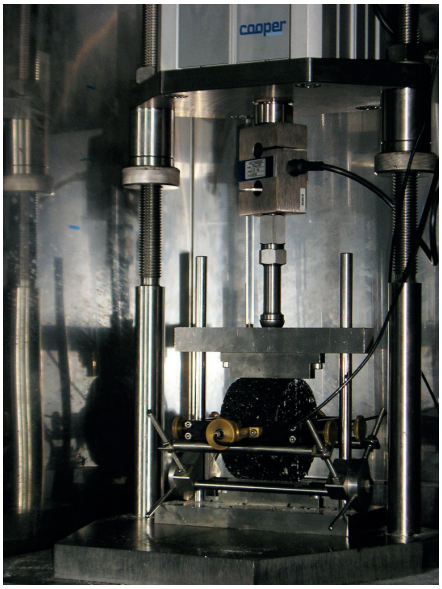


**Fig. 2** Stiffness Modulus test setup

## 3 Methodology

### 3.1 Artificial Neural Networks

ANNs are mathematical models falling in the class of non-linear parametric functions [30]. Such models are the result of the weighted and biased connection of logistic regression units (called artificial neurons), organized in several sequential layers: an input layer that receives the features vector, one or more hidden layers and an output layer that produce the network outcome. The connections, which establish the complexity and computing power of the ANN, link neurons belonging to different layers so that information travels in one direction, but the activity of each neuron is ruled by a non-linear activation function that determines whether the processed output should be transmitted or interrupted. Nonetheless, ANNs are capable to identify the relationship or pattern that links input predictors to target variables because connections' weights and biases are set by a supervised training process that aim to minimize the predicting error of the experimental targets. This study focuses on shallow neural networks (SNNs), i.e., three-layer perceptron networks, which have been shown to solve arbitrarily well any multidimensional input-target fitting problem by providing a sufficient number of neurons in its only hidden layer [31–35, 36]. The proposed SNN consists of a 4-neurons input layer (one neuron for each input feature), a N-neurons hidden layer whose processed output is passed to a hyperbolic tangent (Tanh – Eq. (1)) or exponential linear (ELU – Eq. (2)) activation unit, and a 3-neurons output layer associated with a linear activation.

$$Tanh(x) = \frac{2}{1+e^{-2x}} - 1 \tag{1}$$

$$ELU(x) = \begin{cases} x & x \geq 0 \\ e^{x} - 1 & x < 0 \end{cases} \tag{2}$$

The input features were the bitumen content (% by weight of mix), percentages of aggregate passing at 6.3 mm and 0.063 mm sieves, along with a categorical variable (values: 1 for AC10-5070L, 2 for AC10-SBSL, 3 for AC10-SBSP) that distinguishes the binder type (Standard 50/70 penetration grade vs SBS modified) and the production site (laboratory vs plant). The output variables were IT-CY, AV, and VMA. Each variable has been normalized before being presented to the network, i.e., all the values of a specific variable have been mapped to the range [-1, 1] whose extremes correspond to the minimum and maximum assumed by the feature itself. This reduced computational time and improved the efficiency of the neural model.

### 3.2 ANN training and regularization

The supervised training process identifies connections' weights and biases that minimize the difference between the ANN output $\hat{\boldsymbol{y}}$ and the experimental target $\boldsymbol{y}$, corresponding to the input feature vector $\boldsymbol{x}$. This process is divided into two distinct phases: a forward and a backward pass. In the forward stage, the training feature vector $\boldsymbol{x}$ is inputted to the network and the neurons' activations produce the output $\hat{\boldsymbol{y}}$. After that, a backward comparison is made between the computed output $\hat{\boldsymbol{y}}$ and the experimental target vector $\boldsymbol{y}$ by a performance function $F(\hat{\boldsymbol{y}}, \boldsymbol{y})$, also called loss function, with the aim of defining the corrections to the weights and biases of the network. The training process involves the use of a learning rule that defines the update of network parameters $\boldsymbol{W}$ (the matrix of weights and biases), according to the value assumed by the performance function, for a fixed number of iterations $E$. Mean Squared Error (MSE) is commonly accepted as $F(\cdot)$ function and its gradient with respect to $\boldsymbol{W}$, calculated by means of a backpropagation algorithm, is used in the learning rule so that the network parameters are updated to minimize the loss value. The analytical expression of the learning rule implemented in this study is presented in the Eq. (3). For a generic iteration $e \in \{1,\ldots,E\}$, assuming the Levenberg-Marquardt (LM) backpropagation algorithm [37]:

$$\boldsymbol{W}^{e+1} = \boldsymbol{W}^{e} - \left[\boldsymbol{J}^{T}\left(\boldsymbol{W}^{e}\right)\boldsymbol{J}\left(\boldsymbol{W}^{e}\right) + \mu_{e}\boldsymbol{I}\right]^{-1}\boldsymbol{J}^{T}\left(\boldsymbol{W}^{e}\right)\boldsymbol{v}\left(\boldsymbol{W}^{e}\right), \tag{3}$$

where $\boldsymbol{W}^{e}$ is the matrix of weights and biases at iteration $e$, $\boldsymbol{J}$ is the Jacobian matrix of the training loss $F(\cdot)$ with respect to $\boldsymbol{W}^{e}$, $\boldsymbol{I}$ is the identity matrix and $\boldsymbol{v}(\boldsymbol{W}^{e}) = \hat{\boldsymbol{y}}(\boldsymbol{W}^{e})$ is the vector of network errors. $\boldsymbol{W}^{e+1}$ are the updated values of network parameters to be used in the forward pass of iteration $e + 1$. While the direction towards the minimum is determined by the gradient $\boldsymbol{J}^{T}(\boldsymbol{W}^{e})\boldsymbol{v}(\boldsymbol{W}^{e})$, the scalar $\mu$ determines the step size taken in that direction at each iteration and, as a result, the convergence rate. To achieve faster convergence and to avoid undesirable local minima, the parameter $\mu$ is varied during training: the value $\mu_{e+1}$ corresponds to $\mu_{e}$ multiplied by $\mu_{inc} > 1$ (or $\mu_{dec} < 1$) if the performance index has increased (or decreased) between iterations $e - 1$ and $e$. If the parameter $\mu$ becomes too large, $\mu_{e+1} > \mu_{\max}$, the LM algorithm is stopped. At the end of the $E$ iterations of the training process or when $\mu_{\max}$ is reached, the optimal weights and biases are kept fixed while the test feature vector is processed just in the forward manner to define the model's loss index on novel data. To avoid overfitting caused by too large values of connections' weights

and to improve the performance score on test data, a regularization technique has been implemented in the current study setup [31]. The sum squared error is modified by adding the sum of network weights squares, to penalize network complexity and force the resulting function to be smooth. The ANN optimization objective becomes:

$$F_{opt}\left(\hat{\boldsymbol{y}}\left(\boldsymbol{W}^{e}\right),\boldsymbol{y},\boldsymbol{W}^{e}\right)=\beta\left\|\hat{\boldsymbol{y}}\left(\boldsymbol{W}^{e}\right)-\boldsymbol{y}\right\|_{2}^{2}+\alpha\left\|\boldsymbol{W}^{e}\right\|_{2}^{2}, \quad (4)$$

where the operator $\|\cdot\|_2^2$ represents the 2-norm, applied to the network's parameters $\boldsymbol{W}^e$ and errors $\boldsymbol{v}(\boldsymbol{W}^e) = \hat{\boldsymbol{y}}(\boldsymbol{W}^e)–\boldsymbol{y}$. $\alpha$ and $\beta$ are the regularization parameters that control the complexity of the network solution: the ratio $\alpha/\beta$ assumes values in the interval [0, 1] and the bigger it is, the smoother is the ANN response. T regularization raises the issue of properly setting $\alpha$ and $\beta$ parameters. In this study, David MacKay's approach [38] has been used to optimize the regularization parameters. Hyperparameters that define the functioning of the LM algorithm ($\mu$, $\mu_{inc}$, $\mu_{dec}$, $\mu_{\max}$ and $E$), along with the number of neurons $N$ in the SNN hidden layer and the activation unit type *act*, have been identified by means of a recently introduced Bayesian optimization process [39] that in the current study setup aims to minimize the average MSE index of $k$ trained networks (with the same structure) on a related test data set, as part of a $k$-fold cross validation partitioning.

### 3.3 K-fold cross validation

The standard practice of splitting the available data set into two random subsets of training and testing may result in biased performance evaluations due to the different distribution of data within such splits, along with the risk of missing some relevant trends in training data [40]. These effects are particularly marked when the data set is relatively small. Conversely, the $k$-fold Cross-Validation (CV) method [41] performs a random partition of the experimental observations in $k$ disjointed sub-samples, also called folds, with roughly equal size. Each data fold represents a possible test set, while the remaining $k$–1 are joined together to form the training set. Thereby, k experiments are run and the obtained $k$ test scores are averaged to gain a fair performance evaluation. In the present study, an 8-fold stratified cross-validation was implemented: each randomly identified sub-sample is forced to have roughly the same number of observations for each class of asphalt concrete. Therefore, the 8 folds consist of 12.5% of the available observations, i.e., 4 or 5 for each class of AC.

### 3.4 Hyperparameters optimization

The standard methodologies for the definition of the model's hyperparameters are based on a random or grid search of the combination yielding the lowest score on the loss function. However, these approaches do not allow for an accurate identification of the optimal model and require longer times as the search space becomes larger. Snoek et al. [39] have introduced an automatic hyperparameters search method for machine learning models, based on the Bayesian optimization (BO) process. BO algorithms seek to minimize a given objective function $f(\boldsymbol{h})$ for the hyperparameter vector $\boldsymbol{h}$ in a bounded domain $\mathrm{H} \subset \mathbb{R}$, by fitting a Gaussian process (GP) regression model [42] to the evaluations of $f(\boldsymbol{h})$, i.e., constructing a prior probability distribution of the objective function itself. The GP prior is exploited to make decisions about where in $H$ to evaluate $f(\cdot)$ and, after the result of the experiment with the new set of hyperparameters has been observed, such model is updated to improve its fitting to previous observations. To determine the next point $\boldsymbol{h}_{t+1} \in H$, $t \in \{1,\ldots,T\}$for the evaluation, an acquisition function $\boldsymbol{a}(\boldsymbol{h}_t,\theta) : H \rightarrow \mathbb{R}^+$ is maximized to assess the most suitable combination based on the previously observed samples $\boldsymbol{h}_t$ and the posterior distribution function parameters $\theta$. Among the different existing definitions for $a(\cdot)$, the Expected Improvement (EI) [43] is perhaps the most popular method and has been shown to be efficient in the number of function evaluations required to find the global optimum of many experiments [44, 45]. Such EI acquisition function evaluates the expected amount of improvement in $f(\cdot)$. To escape a local minimum, the improvement proposed by Bull [45] allows the EI acquisition function to modify its behaviour when it estimates the over-exploitation of an area of surface $f(\cdot)$. Thanks to this enhancement, such acquisition function is called Expected-Improvement-Plus (EIP) [46]. Given the seven hyperparameters $N$, *act*, $\mu$, $\mu_{inc}$, $\mu_{dec}$, $\mu_{\max}$, $E$ and their bounded domain (Table 3), $f(\cdot)$ is a function that constructs a SNN with $N$ neurons in the hidden layer, *act* as activation function and runs an 8-Fold CV experiment in which the network is trained on eight disjointed data sets for $E$ iterations with an adaptive learning step size $\mu$. $\alpha$ and $\beta$ are updated iteratively by an independent procedure [41] to force the resulting interpolation to be smooth. $f(\cdot)$ returns a single scalar that express the average MSE obtained by the SNNs on the 8-related test folds. The Bayesian optimization algorithm is run for 150 iterations.

**Table 3** Summary of Bayesian optimization

| Feature | Bounded Domain | Selected Value |
|---|---|---|
| $N$ | {8,…,64} | 22 |
| $act$ | {*Tanh*, *ELU*} | *Tanh* |
| $\mu$ | $[10^{-4}, 10^{-2}]$ | $2.02 \times 10^{-3}$ |
| $\mu_{inc}$ | $[10^{1}, 10^{3}]$ | $1.18 \times 10^{2}$ |
| $\mu_{dec}$ | $[10^{-3}, 10^{-1}]$ | $1.07 \times 10^{-2}$ |
| $\mu_{\max}$ | $[10^{6}, 10^{8}]$ | $4.52 \times 10^{7}$ |
| $E$ | {500,…,5000} | 2922 |

The brackets {·} are used for the integer or categorical ranges and the brackets [·] are used for variables searched on a log scale

## 4 Results and discussion

The first attempt combination $\boldsymbol{h}_0$ was assigned in order to make the procedure replicable and corresponded to: $N$=10, $act$=*Tanh*, $\mu$=1*e*–3, $\mu_{inc}$=1*e*1, $\mu_{dec}$=1*e*–1, $\mu_{\max}$=1*e*8, $E$ = 1000. Fig. 3 shows in a dispersion diagram the MSE scores averaged over the 8 test folds for each of the 150 experiments in the optimization process. Although the search space defined by the bounded domains was quite large, the set of hyperparameters that minimized the prediction error on the 8 folds was detected at iteration 77 (i.e., about at half of the expected iterations) and it was characterized by $N$ = 22 neurons in the hidden layer and an $act$ = *Tanh* transfer function. Such neural network was trained according to the LM algorithm for $E$ = 2922 iterations with an initial learning step size $\mu_0$ = 0.00202. The parameter $\mu$ was modified at each iteration by $\mu_{inc}$ = 1.18*e*2 or $\mu_{dec}$ = 1.07*e*–2 to reduce the convergence time and to avoid local minima. The training process was stopped when the maximum number of iterations was reached or $\mu_{\max}$ = 4.52*e*7 which denoted the convergence of the regularization process. Alternatively, Bayesian optimization procedure could have been applied iteratively, setting a sufficiently large first attempt search space (so as not to require excessive computational time), and then expand or reduce the variability range of one or more hyperparameters to evaluate its effect on the solution.

A further consideration can be made by looking at Fig. 3. When the minimum error has been reached (at iteration 77), the BO algorithm continued to look for an improving-performance combination around the point $\boldsymbol{h}_{77}$. After a few iterations in which no new minimum has been found, the mean square error increased almost suddenly due to the acquisition of a set of hyperparameters far from the minimum point. This happened thanks to the improvement proposed by Bull [45] to the EI acquisition function: the EIP function estimated an over-exploration of

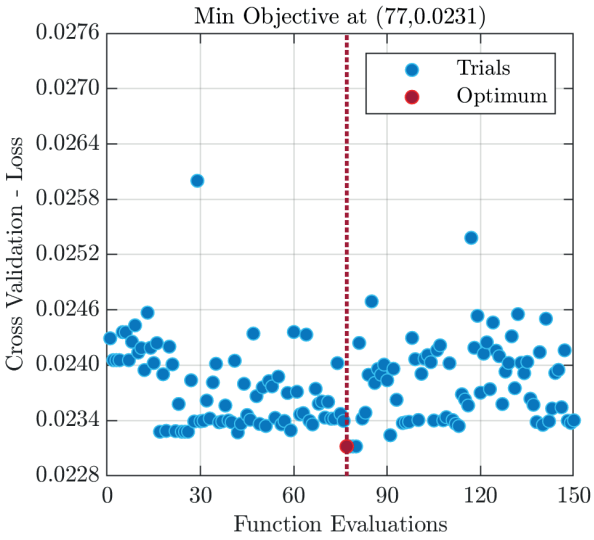


**Fig. 3** Observed average MSE-score on the 8 test folds versus the number of function evaluations

the error surface area near the minimum and moved elsewhere, randomly selecting a new combination of hyperparameters. The test results of the optimal SNN model for each of the 8 folds, relating to the MSE and the Pearson correlation coefficient ($R$) between the experimental targets and the network outputs, are shown in Table 4. In particular, the  score is specified for each of the 3 output variables of the neural model, i.e., IT-CY, AV, and VMA. The shallow neural network identified by the BO process produced a good spatial interpolation, giving a satisfactory prediction of both the stiffness ($R_{IT\text{–}CY} \geq 0.8698$) and the main volumetric properties ($R_{AV} \geq 0.8826$, $R_{VMA} \geq 0.8470$) of asphalt concrete for thin layers. The fluctuations of the MSE index on the 8 folds (second column in Table 4) are caused by the different distribution of training and test data. Therefore, the implementation of a cross-validation in the procedure was effective to avoid a biased evaluation of the model performance. The last row of Table 4 shows the SNN actual generalization characteristics for the modeling problem covered by this study, obtained by averaging the results over the 8 folds. Hence, the correlation coefficient can be properly evaluated:

$$R_{mean} = \left(0.9544 + 0.9519 + 0.9407\right) / 3 = 0.9490 \,. \qquad (5)$$

Although asphalt concretes have quite different characteristics, the optimal BO model gives satisfactory results on all the 8 folds: the worst $R$ score (fold 5) was , while the best one (fold 8) was . Fig. 4 shows graphically an example of the correlation analysis between targets and outputs obtained for the folds just mentioned. These are significant engineering findings because they show how SNNs

can simultaneously model mechanical and physical properties of bituminous mixtures widely different in composition and production site.

**Table 4** Mean Squared Error and Pearson coefficient results

| Fold | Loss (MSE) | R-Pearson coefficient | | |
|---|---|---|---|---|
| | | IT-CY | AV | VMA |
| 1 | 0.0172 | 0.9780 | 0.9523 | 0.9374 |
| 2 | 0.0318 | 0.9654 | 0.9332 | 0.9204 |
| 3 | 0.0181 | 0.9952 | 0.9413 | 0.9535 |
| 4 | 0.0273 | 0.9109 | 0.9746 | 0.9630 |
| 5 | 0.0520 | 0.8698 | 0.8826 | 0.8470 |
| 6 | 0.0130 | 0.9856 | 0.9863 | 0.9674 |
| 7 | 0.0209 | 0.9569 | 0.9470 | 0.9440 |
| 8 | 0.0047 | 0.9731 | 0.9975 | 0.9931 |
| Result – Average on the 8 test folds | | | | |
| | 0.0231 | 0.9544 | 0.9519 | 0.9407 |

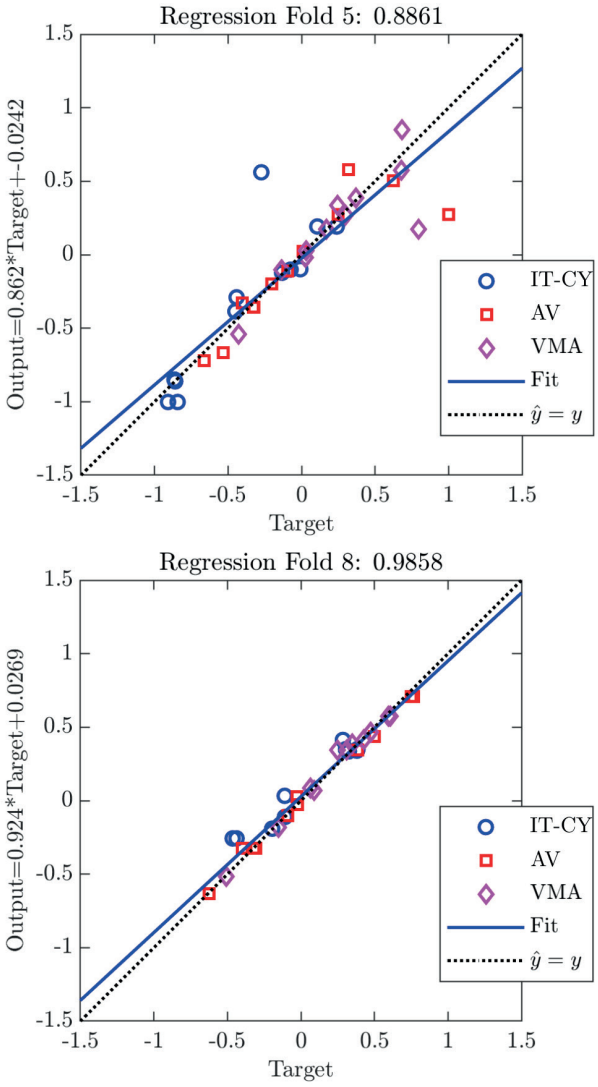


**Fig. 4** Regression analysis on fold 5 (up) and on fold 8 (down)

## 5 Conclusions

The development of a performance-based road pavement mix design method requires the definition of innovative procedures for the analysis of experimental data, which can efficiently produce reliable predictive models of the asphalt concrete response. In such a context, ANNs represent a useful regression technique, but they pose the problem of determining the parametric and structural components that define their optimal functioning for the modeling problem addressed. Bayesian optimization represents a novel procedure able to independently set the optimal hyperparameters of a SNN and to reliably evaluate the generalization feature of a proposed model. This procedure combines several well-established methods in the scientific field and is applicable to any modeling problem, downstream of a careful experimentation. The presented approach mainly exploits the k-fold CV, to average the prediction error of a model on k independent datasets, and the Bayesian optimization, to build a posterior probability distribution of the error function (based on past evaluations of certain hyperparameter sets) to be used to identify a next hyperparameter combination (to be tested) that can improve the predictive feature of a model (i.e., maximizing the probability). The proposed methodology was verified by adopting as a case study the modeling of the mechanical response and volumetric properties of 92 specimens of road pavement asphalt concrete for thin wearing layers on the basis of the main compositional variables of the mixture, such as the bitumen content (% by weight of mix), percentages of aggregate passing at 6.3 mm and 0.063 mm sieves, along with a categorical variable that distinguishes the binder type (Standard 50/70 penetration grade vs SBS modified) and the production site (laboratory vs plant). The output variables were the stiffness modulus, the air voids and the voids in the mineral aggregate. Findings confirmed that the classical modeling approach may lead to biased assessments of the model's generalization feature. Therefore, cross-validation is essential to evaluate the actual performance of the model, especially when there are few available observations of the phenomenon. In addition, the Bayesian process successfully identified the optimal combination of hyperparameters leading to a smooth interpolation function of the training data, characterized by an average Pearson coefficient on $k = 8$ folds equal to $R_{mean} = 0.9490$. Such an optimal model selection process is more rational, objective and efficient than classic time-consuming hyperparameters fine-tuning procedures (as grid or random search). However, the

result of Bayesian optimization may depend on the hyperparameters variability ranges, fixed by the research civil engineer, which create constraints to the solution search space. In the study setup, the intervals were taken quite large to avoid errors in the selection of the optimal model. The presented approach was explained in detail to give the reader an opportunity to replicate it. However, the network properties set out above may be different if the proposed procedure is applied to a different experimental data set. The model developed in this study, although it gives excellent predicting results, can be applied within the limits imposed by the maximum and minimum values of the input variables considered. Therefore, it needs future developments to increase the number of aggregate gradations of asphalt concretes for thin wearing layers and the bitumen content values of the plant-produced mixes. A further contribution to the performance-based mix design could come from the use of fatigue or permanent deformation resistance as modeling variables. Finally, deep learning modeling approaches could be investigated in the future to investigate more complex relationships between input and target variables and to determine whether they are preferable to shallow neural ones in terms of performance and computational effort.

## References

[1] Alavi, A. H., Ameri, M., Gandomi, A. H., Mirzahosseini, M. R. "Formulation of flow number of asphalt mixes using a hybrid computational method", Construction and Building Materials, 25(3), pp. 1338–1355, 2011. https://doi.org/10.1016/j.conbuildmat.2010.09.010

[2] Wang, L., Gong, H., Hou, Y., Shu, X., Huang, B. "Advances in pavement materials, design, characterisation, and simulation", Road Materials and Pavement Design, 18(S3), pp. 1–11, 2017. https://doi.org/10.1080/14680629.2017.1329856

[3] Pasetto, M., Baldo, N. "Numerical visco-elastoplastic constitutive modelization of creep recovery tests on hot mix asphalt", Journal of Traffic and Transportation Engineering (English Edition), 3(5), pp. 390–397, 2016. https://doi.org/10.1016/j.jtte.2016.09.009

[4] Montoya, M. A., Haddock, J. E. "Estimating asphalt mixture volumetric properties using seemingly unrelated regression equations approaches", Construction and Building Materials, 225, pp. 829–837, 2019. https://doi.org/10.1016/j.conbuildmat.2019.07.266

[5] Ozsahin, T. S., Oruc, S. "Neural network model for resilient modulus of emulsified asphalt mixtures", Construction and Building Materials, 22(7), pp. 1436–1445, 2008. https://doi.org/10.1016/j.conbuildmat.2007.01.031

[6] Tapkın, S., Çevik, A., Uşar, Ü. "Accumulated strain prediction of polypropylene modified marshall specimens in repeated creep test using artificial neural networks", Expert Systems with Applications, 36(8), pp. 11186–11197, 2009. https://doi.org/10.1016/j.eswa.2009.02.089

[7] Mirzahosseini, M. R., Aghaeifar, A., Alavi, A. H., Gandomi, A. H., Seyednour, R. "Permanent deformation analysis of asphalt mixtures using soft computing techniques", Expert Systems with Applications, 8(5), pp. 6081–6100, 2011. https://doi.org/10.1016/j.eswa.2010.11.002

[8] Xiao, F., Amirkhanian, S., Juang, C. H. "Prediction of fatigue life of rubberized asphalt concrete mixtures containing reclaimed asphalt pavement using artificial neural networks", Journal of Materials in Civil Engineering, 21(6), pp. 253–261, 2009. https://doi.org/10.1061/(ASCE)0899-1561(2009)21:6(253)

[9] Ahmed, T. M., Green, P. L., Khalid, H. A. "Predicting fatigue performance of hot mix asphalt using artificial neural networks", Road Materials and Pavement Design, 18(sup2), pp. 141–154, 2017. https://doi.org/10.1080/14680629.2017.1306928

[10] Ceylan, H., Schwartz, C. W., Kim, S., Gopalakrishnan, K. "Accuracy of predictive models for dynamic modulus of hot-mix asphalt", Journal of Materials in Civil Engineering, 21(6), pp. 286–293, 2009. https://doi.org/10.1061/(ASCE)0899-1561(2009)21:6(286)

[11] Zavrtanik, N., Prosen, J., Tušar, M., Turk, G. "The use of artificial neural networks for modeling air void content in aggregate mixture", Automation in Construction, 63, pp. 155–161, 2016. https://doi.org/10.1016/j.autcon.2015.12.009

[12] Androjić, I., Marović, I. "Development of artificial neural network and multiple linear regression models in the prediction process of the hot mix asphalt properties", Canadian Journal of Civil Engineering, 44(12), pp. 994–1004, 2017. https://doi.org/10.1139/cjce-2017-0300

[13] Baldo, N., Manthos, E., Miani, M. "Stiffness modulus and Marshall parameters of hot mix asphalts: laboratory data modeling by artificial neural networks characterized by cross-validation", Applied Sciences, 9(17), 3502, 2019. https://doi.org/10.3390/app9173502

[14] Shahriari, B., Swersky, K., Wang, Z., Adams, R. P., de Freitas, N. "Taking the human out of the loop: A review of Bayesian optimization", Proceedings of the Institution of Electrical Engineers, 104(1), pp. 148–175, 2016. https://doi.org/10.1109/JPROC.2015.2494218

[15] Bergstra, J., Bardenet, R., Bengio, Y., Kégl, B. "Algorithms for hyper-parameter optimization", In: Shawe-Taylor, J., Zemal, R., Bartlett, P., Pereira, F., Weinberger, K. Q. (eds.) Advances in Neural Information Processing Systems 24 (NIPS 2011), Neural Information Processing Systems Foundation, Inc., 2011. ISBN: 9781618395993 [online] Available at: https://papers.nips.cc/paper/2011/file/86e8f7ab32cfd12577bc2619bc635690-Paper.pdf

[16] Bergstra, J., Yamins, D., Cox, D. D. "Making a science of model search: Hyperparameter optimization in hundreds of dimensions for vision architectures", [pdf] In: Proceedings of the 30th International Conference on Machine Learning, Atlanta, GA, USA, 2013, pp. 115–123. Available at: https://proceedings.mlr.press/v28/bergstra13.html

[17] CEN "EN 13108-2:2016 Bituminous mixtures - Material specifications - Part 2: Asphalt Concrete for Very Thin Layers (BBTM)", European Committee for Standardization, Brussels, Belgium, 2016.
[18] CEN "EN 1097-2:2020 Tests for mechanical and physical properties of aggregates - Part 2: Methods for the determination of resistance to fragmentation", European Committee for Standardization, Brussels, Belgium, 2020.
[19] CEN "EN 1097-8:2020 Tests for mechanical and physical properties of aggregates - Part 8: Determination of the polished stone value", European Committee for Standardization, Brussels, Belgium, 2020.
[20] CEN "EN 933-3:2012 Tests for geometrical properties of aggregates - Part 3: Determination of particle shape - Flakiness index", European Committee for Standardization, Brussels, Belgium, 2012.
[21] CEN "EN 933-8 :2012+A1:2015 Tests for geometrical properties of aggregates - Part 8: Assessment of fines - Sand equivalent test", European Committee for Standardization, Brussels, Belgium, 2015.
[22] CEN "EN 933-9:2022 Tests for geometrical properties of aggregates - Part 9: Assessment of fines - Methylene blue test", European Committee for Standardization, Brussels, Belgium, 2022.
[23] CEN "EN 1426:2015 Bitumen and bituminous binders - Determination of needle penetration", European Committee for Standardization, Brussels, Belgium, 2015.
[24] CEN "EN 1427:2015 Bitumen and bituminous binders - Determination of the softening point - Ring and Ball method", European Committee for Standardization, Brussels, Belgium, 2015.
[25] CEN "EN 13398:2017 Bitumen and bituminous binders - Determination of the elastic recovery of modified bitumen", European Committee for Standardization, Brussels, Belgium, 2017.
[26] CEN "EN 12593:2015 Bitumen and bituminous binders - Determination of the Fraass breaking point", European Committee for Standardization, Brussels, Belgium, 2015.
[27] CEN "EN 12697-30:2018 Bituminous mixtures - Test methods - Part 30: Specimen preparation by impact compactor", European Committee for Standardization, Brussels, Belgium, 2018.
[28] CEN "EN 12697-8:2019 Bituminous mixtures - Test methods - Part 8: Determination of void characteristics of bituminous specimens", European Committee for Standardization, Brussels, Belgium, 2019.
[29] CEN "EN 12697-26:2018 Bituminous mixtures - Test methods - Part 26: Stiffness", European Committee for Standardization, Brussels, Belgium, 2018.
[30] McCulloch, W. S., Pitts, W. "A logical calculus of the ideas immanent in nervous activity", In: Anderson, J. A., Rosenfeld, E. (eds.) Neurocomputing: Foundations of Research, MIT Press, 1988, pp. 15–27. ISBN:978-0-262-01097-9 [online] Available at: http://dl.acm.org/citation.cfm?id=65669.104377
[31] Hagan, M. T., Demuth, H. B., Beale, M. H., De Jesús, O. "Function Approximation", In: Neural Network Design, 2nd ed., PWS Publishing, 2014, pp. (11)4–7. ISBN: 978-0-9717321-1-7
[32] Hagan, M. T., Demuth, H. B., Beale, M. H., De Jesús, O. "Levenberg-Marquardt Algorithm", In: Neural Network Design, 2nd ed., PWS Publishing, 2014, pp. (12)19–27. ISBN: 978-0-9717321-1-7
[33] Hagan, M. T., Demuth, H. B., Beale, M. H., De Jesús, O. "Regularization", In: Neural Network Design, 2nd ed., PWS Publishing, 2014, pp. (13)8–10. ISBN: 978-0-9717321-1-7
[34] Hagan, M. T., Demuth, H. B., Beale, M. H., De Jesús, O. "Bayesian Analysis", In: Neural Network Design, 2nd ed., PWS Publishing, 2014, pp. (13)10–12. ISBN: 978-0-9717321-1-7
[35] Hagan, M. T., Demuth, H. B., Beale, M. H., De Jesús, O. "Bayesian Regularization, Relationship Between Early Stopping and Regularization", In: Neural Network Design, 2nd ed., PWS Publishing, 2014, pp. (13)12–19. ISBN: 978-0-9717321-1-7
[36] Tiwari, N., Baldo, N., Satyam, N., Miani, M. "Mechanical Characterization of Industrial Waste Materials as Mineral Fillers in Asphalt Mixes: Integrated Experimental and Machine Learning Analysis", Sustainability, 14(10), 5946, 2022. https://doi.org/10.3390/su14105946
[37] Hagan, M. T., Menhaj, M. B. "Training feed-forward networks with the Marquardt algorithm", IEEE Transactions on Neural Networks, 5(6), pp. 989–993, 1994. https://doi.org/10.1109/72.329697
[38] MacKay, D. J. C. "Bayesian Interpolation", Neural Computation, 4(3), pp. 415–447, 1992. https://doi.org/10.1162/neco.1992.4.3.415
[39] Snoek, J., Larochelle, H., Adams, R. P. "Practical Bayesian Optimization of Machine Learning Algorithms", In: Proceedings of the 25th International Conference on Neural Information Processing Systems (NIPS), Lake Tahoe, NV, USA, 2012, pp. 2951–2959. [online] Available at: http://papers.nips.cc/paper/4522-practical-bayesian-optimization
[40] Miani, M., Dunnhofer, M., Rondinella, F., Manthos, E., Valentin, J., Micheloni, C., Baldo, N. "Bituminous Mixtures Experimental Data Modeling Using a Hyperparameters-Optimized Machine Learning Approach", Applied Sciences, 11(24), 11710, 2021. https://doi.org/10.3390/app112411710
[41] James, G., Witten, D., Hastie, T., Tibshirani, R. "Cross-Validation", In: Casella, G., Fienberg, S., Olkin, I. (eds.) An Introduction to Statistical Learning: With Applications in R, Springer, 2013, pp. 176–186. ISBN: 978-1461471370
[42] Rasmussen, C. E., Williams, C. K. I. "Gaussian Processes for Machine Learning", 2nd ed., MIT Press, 2006, pp. 105-118. ISBN 0-262-18253-X [online] Available at: http://www.gaussianprocess.org/gpml/
[43] Mockus, J., Tiešis, V., Zilinskas, A. "The application of Bayesian methods for seeking the extremum", In: Dixon, L. C. W, Szego, G. P. (eds.) Towards Global Optimization 2, North Holland Publishing, 1978, pp. 117–129. ISBN: 0444851712
[44] Srinivas, N., Krause, A., Kakade, S., Seeger, M. "Gaussian Process Optimization in the Bandit Setting: No Regret and Experimental Design", In: Proceedings of the 27th International Conference on Machine Learning (ICML), Haifa, Israel, 2010, pp. 1015–1022. [online] Available at: http://dl.acm.org/citation.cfm?id=3104322.3104451
[45] Bull, A. D. "Convergence rates of efficient global optimization algorithms", [stat.ML] arXiv:1101.3501, Journal of Machine Learning Research, 12, pp. 2879–2904, 2011. https://doi.org/10.48550/arXiv.1101.3501
[46] Baldo, N., Miani, M., Rondinella, F., Valentin, J., Vackcová, P., Manthos, E. "Stiffness Data of High-Modulus Asphalt Concretes for Road Pavements: Predictive Modeling by Machine-Learning", Coatings, 12(1), 54, 2022. https://doi.org/10.3390/coatings12010054

## Appendix A

**Table 5** Specimens' bitumen content, respective volumetric properties, and Stiffness Modulus results

| Specimen | Stiffness at 20°C(MPa) | Air voids (%) | V.M.A (%) | Bitumen content (% by weight of mix) | Filler to bitumen ratio | V.F.A (%) | Percentage Passing (%) at | | | | | Categories |
|---|---|---|---|---|---|---|---|---|---|---|---|---|
| | | | | | | | 10 mm sieve | 6.3 mm sieve | 2 mm sieve | 0.5 mm sieve | 0.063 mm sieve | |
| 1 | 2939 | 15.7 | 23.3 | 4.12 | 1.30 | 32.5 | 93.54 | 31.84 | 26.99 | 13.23 | 5.35 | 1 |
| 2 | 2708 | 15.9 | 23.5 | 4.12 | 1.30 | 32.2 | 93.54 | 31.84 | 26.99 | 13.23 | 5.35 | 1 |
| 3 | 2944 | 15.4 | 23.0 | 4.12 | 1.30 | 33.0 | 93.54 | 31.84 | 26.99 | 13.23 | 5.35 | 1 |
| 4 | 2445 | 14.2 | 23.2 | 4.76 | 1.12 | 38.7 | 93.54 | 31.84 | 26.99 | 13.23 | 5.35 | 1 |
| 5 | 2586 | 14.2 | 23.1 | 4.76 | 1.12 | 38.8 | 93.54 | 31.84 | 26.99 | 13.23 | 5.35 | 1 |
| 6 | 2441 | 14.9 | 23.8 | 4.76 | 1.12 | 37.4 | 93.54 | 31.84 | 26.99 | 13.23 | 5.35 | 1 |
| 7 | 1962 | 11.1 | 21.7 | 5.39 | 0.99 | 48.7 | 93.54 | 31.84 | 26.99 | 13.23 | 5.35 | 1 |
| 8 | 1945 | 11.3 | 21.8 | 5.39 | 0.99 | 48.2 | 93.54 | 31.84 | 26.99 | 13.23 | 5.35 | 1 |
| 9 | 1921 | 11.6 | 22.1 | 5.39 | 0.99 | 47.4 | 93.54 | 31.84 | 26.99 | 13.23 | 5.35 | 1 |
| 10 | 1775 | 9.3 | 21.3 | 6.02 | 0.89 | 56.5 | 93.54 | 31.84 | 26.99 | 13.23 | 5.35 | 1 |
| 11 | 1886 | 9.4 | 21.4 | 6.02 | 0.89 | 56.2 | 93.54 | 31.84 | 26.99 | 13.23 | 5.35 | 1 |
| 12 | 1965 | 9.4 | 21.4 | 6.02 | 0.89 | 56.2 | 93.54 | 31.84 | 26.99 | 13.23 | 5.35 | 1 |
| 13 | 3276 | 12.7 | 20.6 | 4.12 | 1.39 | 38.2 | 93.90 | 35.62 | 30.75 | 13.88 | 5.71 | 1 |
| 14 | 3116 | 17.1 | 24.5 | 4.12 | 1.39 | 30.4 | 93.90 | 35.62 | 30.75 | 13.88 | 5.71 | 1 |
| 15 | 3227 | 12.7 | 20.6 | 4.12 | 1.39 | 38.1 | 93.90 | 35.62 | 30.75 | 13.88 | 5.71 | 1 |
| 16 | 2760 | 9.6 | 19.1 | 4.76 | 1.20 | 49.6 | 93.90 | 35.62 | 30.75 | 13.88 | 5.71 | 1 |
| 17 | 2750 | 11.6 | 20.8 | 4.76 | 1.20 | 44.4 | 93.90 | 35.62 | 30.75 | 13.88 | 5.71 | 1 |
| 18 | 2749 | 10.7 | 20.1 | 4.76 | 1.20 | 46.5 | 93.90 | 35.62 | 30.75 | 13.88 | 5.71 | 1 |
| 19 | 2399 | 9.3 | 20.1 | 5.39 | 1.06 | 53.6 | 93.90 | 35.62 | 30.75 | 13.88 | 5.71 | 1 |
| 20 | 2355 | 10.2 | 20.8 | 5.39 | 1.06 | 51.2 | 93.90 | 35.62 | 30.75 | 13.88 | 5.71 | 1 |
| 21 | 2336 | 7.1 | 18.2 | 5.39 | 1.06 | 60.7 | 93.90 | 35.62 | 30.75 | 13.88 | 5.71 | 1 |
| 22 | 1939 | 7.4 | 19.7 | 6.02 | 0.95 | 62.3 | 93.90 | 35.62 | 30.75 | 13.88 | 5.71 | 1 |
| 23 | 1964 | 8.6 | 20.7 | 6.02 | 0.95 | 58.4 | 93.90 | 35.62 | 30.75 | 13.88 | 5.71 | 1 |
| 24 | 1956 | 5.5 | 18.0 | 6.02 | 0.95 | 69.7 | 93.90 | 35.62 | 30.75 | 13.88 | 5.71 | 1 |
| 25 | 2421 | 9.4 | 20.0 | 5.35 | 1.07 | 53.2 | 93.90 | 35.62 | 30.75 | 13.88 | 5.71 | 1 |
| 26 | 2354 | 10.2 | 20.8 | 5.35 | 1.07 | 50.9 | 93.90 | 35.62 | 30.75 | 13.88 | 5.71 | 1 |
| 27 | 2342 | 7.2 | 18.1 | 5.35 | 1.07 | 60.3 | 93.90 | 35.62 | 30.75 | 13.88 | 5.71 | 1 |
| 28 | 1965 | 7.4 | 19.7 | 6.00 | 0.95 | 62.1 | 93.90 | 35.62 | 30.75 | 13.88 | 5.71 | 1 |
| 29 | 1957 | 8.7 | 20.7 | 6.00 | 0.95 | 58.2 | 93.90 | 35.62 | 30.75 | 13.88 | 5.71 | 1 |
| 30 | 1948 | 5.5 | 18.0 | 6.00 | 0.95 | 69.5 | 93.90 | 35.62 | 30.75 | 13.88 | 5.71 | 1 |
| 31 | 3197 | 15.6 | 24.5 | 4.41 | 1.20 | 36.5 | 92.10 | 33.87 | 26.15 | 13.03 | 5.30 | 2 |
| 32 | 3067 | 17.0 | 25.8 | 4.41 | 1.20 | 34.1 | 92.10 | 33.87 | 26.15 | 13.03 | 5.30 | 2 |
| 33 | 3278 | 16.4 | 25.3 | 4.41 | 1.20 | 35.1 | 92.10 | 33.87 | 26.15 | 13.03 | 5.30 | 2 |
| 34 | 3066 | 15.6 | 15.6 | 4.79 | 1.11 | 38.3 | 92.10 | 33.87 | 26.15 | 13.03 | 5.30 | 2 |
| 35 | 3044 | 16.3 | 16.3 | 4.79 | 1.11 | 37.2 | 92.10 | 33.87 | 26.15 | 13.03 | 5.30 | 2 |
| 36 | 2931 | 13.2 | 13.2 | 4.79 | 1.11 | 43.0 | 92.10 | 33.87 | 26.15 | 13.03 | 5.30 | 2 |
| 37 | 2840 | 14.4 | 24.9 | 5.11 | 1.04 | 42.3 | 92.10 | 33.87 | 26.15 | 13.03 | 5.30 | 2 |
| 38 | 2976 | 13.1 | 23.8 | 5.11 | 1.04 | 45.0 | 92.10 | 33.87 | 26.15 | 13.03 | 5.30 | 2 |
| 39 | 2873 | 15.0 | 25.5 | 5.11 | 1.04 | 41.0 | 92.10 | 33.87 | 26.15 | 13.03 | 5.30 | 2 |
| 40 | 3226 | 11.9 | 23.5 | 5.48 | 0.97 | 49.4 | 92.10 | 33.87 | 26.15 | 13.03 | 5.30 | 2 |
| 41 | 2928 | 13.2 | 24.6 | 5.48 | 0.97 | 46.5 | 92.10 | 33.87 | 26.15 | 13.03 | 5.30 | 2 |
| 42 | 3093 | 12.6 | 24.1 | 5.48 | 0.97 | 47.8 | 92.10 | 33.87 | 26.15 | 13.03 | 5.30 | 2 |
| 43 | 3123 | 10.9 | 23.4 | 5.86 | 0.96 | 53.5 | 93.54 | 31.84 | 26.99 | 13.65 | 5.60 | 2 |
| 44 | 3091 | 10.9 | 23.5 | 5.86 | 0.96 | 53.4 | 93.54 | 31.84 | 26.99 | 13.65 | 5.60 | 2 |

Continuation of Table 5

| | | | | | | | | | | | | |
|---|---|---|---|---|---|---|---|---|---|---|---|---|
| 45 | 3358 | 12.3 | 24.6 | 5.86 | 0.96 | 50.1 | 93.54 | 31.84 | 26.99 | 13.65 | 5.60 | 2 |
| 46 | 3452 | 15.6 | 23.2 | 4.12 | 1.36 | 32.8 | 93.54 | 31.84 | 26.99 | 13.65 | 5.60 | 2 |
| 47 | 3356 | 15.7 | 23.3 | 4.12 | 1.36 | 32.7 | 93.54 | 31.84 | 26.99 | 13.65 | 5.60 | 2 |
| 48 | 3384 | 15.3 | 23.0 | 4.12 | 1.36 | 33.3 | 93.54 | 31.84 | 26.99 | 13.65 | 5.60 | 2 |
| 49 | 3105 | 14.1 | 23.1 | 4.76 | 1.18 | 39.0 | 93.54 | 31.84 | 26.99 | 13.65 | 5.60 | 2 |
| 50 | 3085 | 13.9 | 23.0 | 4.76 | 1.18 | 39.4 | 93.54 | 31.84 | 26.99 | 13.65 | 5.60 | 2 |
| 51 | 3078 | 14.2 | 23.2 | 4.76 | 1.18 | 38.8 | 93.54 | 31.84 | 26.99 | 13.65 | 5.60 | 2 |
| 52 | 2856 | 11.1 | 21.7 | 5.39 | 1.04 | 48.8 | 93.54 | 31.84 | 26.99 | 13.65 | 5.60 | 2 |
| 53 | 2854 | 11.1 | 21.7 | 5.39 | 1.04 | 48.9 | 93.54 | 31.84 | 26.99 | 13.65 | 5.60 | 2 |
| 54 | 2841 | 11.2 | 21.8 | 5.39 | 1.04 | 48.5 | 93.54 | 31.84 | 26.99 | 13.65 | 5.60 | 2 |
| 55 | 2424 | 8.9 | 21.1 | 6.02 | 0.93 | 57.6 | 93.54 | 31.84 | 26.99 | 13.65 | 5.60 | 2 |
| 56 | 2451 | 8.9 | 21.0 | 6.02 | 0.93 | 57.6 | 93.54 | 31.84 | 26.99 | 13.65 | 5.60 | 2 |
| 57 | 2456 | 9.4 | 21.5 | 6.02 | 0.93 | 56.2 | 93.54 | 31.84 | 26.99 | 13.65 | 5.60 | 2 |
| 58 | 2422 | 7.9 | 20.4 | 6.10 | 0.92 | 61.0 | 93.54 | 31.84 | 26.99 | 13.65 | 5.60 | 2 |
| 59 | 2438 | 8.6 | 21.0 | 6.10 | 0.92 | 58.8 | 93.54 | 31.84 | 26.99 | 13.65 | 5.60 | 2 |
| 60 | 2468 | 8.6 | 20.9 | 6.10 | 0.92 | 58.9 | 93.54 | 31.84 | 26.99 | 13.65 | 5.60 | 2 |
| 61 | 3382 | 9.5 | 18.5 | 5.58 | 1.01 | 48.9 | 92.10 | 33.87 | 26.15 | 13.03 | 5.63 | 3 |
| 62 | 3446 | 9.3 | 18.3 | 5.58 | 1.01 | 49.2 | 92.10 | 33.87 | 26.15 | 13.03 | 5.63 | 3 |
| 63 | 3260 | 9.6 | 18.7 | 5.58 | 1.01 | 48.6 | 92.10 | 33.87 | 26.15 | 13.03 | 5.63 | 3 |
| 64 | 3617 | 9.1 | 18.1 | 5.58 | 1.01 | 49.7 | 92.10 | 33.87 | 26.15 | 13.03 | 5.63 | 3 |
| 65 | 3362 | 14.1 | 22.5 | 5.27 | 1.11 | 37.2 | 97.73 | 31.17 | 23.17 | 13.82 | 5.87 | 3 |
| 66 | 3458 | 13.5 | 22.2 | 5.27 | 1.11 | 39.0 | 97.73 | 31.17 | 23.17 | 13.82 | 5.87 | 3 |
| 67 | 3421 | 13.9 | 22.3 | 5.27 | 1.11 | 37.6 | 97.73 | 31.17 | 23.17 | 13.82 | 5.87 | 3 |
| 68 | 3380 | 13.9 | 22.7 | 5.27 | 1.11 | 39.0 | 97.73 | 31.17 | 23.17 | 13.82 | 5.87 | 3 |
| 69 | 2810 | 10.3 | 19.5 | 5.47 | 1.06 | 47.3 | 92.81 | 32.02 | 24.14 | 15.84 | 5.77 | 3 |
| 70 | 2842 | 10.0 | 18.5 | 5.47 | 1.06 | 45.9 | 92.81 | 32.02 | 24.14 | 15.84 | 5.77 | 3 |
| 71 | 2826 | 10.1 | 18.6 | 5.47 | 1.06 | 46.0 | 92.81 | 32.02 | 24.14 | 15.84 | 5.77 | 3 |
| 72 | 2827 | 10.1 | 18.6 | 5.47 | 1.06 | 46.0 | 92.81 | 32.02 | 24.14 | 15.84 | 5.77 | 3 |
| 73 | 2655 | 8.2 | 16.8 | 5.74 | 1.07 | 51.4 | 92.05 | 33.50 | 24.00 | 13.98 | 6.12 | 3 |
| 74 | 3940 | 7.1 | 15.9 | 5.74 | 1.07 | 55.0 | 92.05 | 33.50 | 24.00 | 13.98 | 6.12 | 3 |
| 75 | 3612 | 7.4 | 16.1 | 5.74 | 1.07 | 54.1 | 92.05 | 33.50 | 24.00 | 13.98 | 6.12 | 3 |
| 76 | 3448 | 7.6 | 16.3 | 5.74 | 1.07 | 53.2 | 92.05 | 33.50 | 24.00 | 13.98 | 6.12 | 3 |
| 77 | 3332 | 13.5 | 22.2 | 5.29 | 1.05 | 39.2 | 93.24 | 35.00 | 22.35 | 13.28 | 5.58 | 3 |
| 78 | 3388 | 13.3 | 21.6 | 5.29 | 1.05 | 38.4 | 93.24 | 35.00 | 22.35 | 13.28 | 5.58 | 3 |
| 79 | 3316 | 13.6 | 22.4 | 5.29 | 1.05 | 39.3 | 93.24 | 35.00 | 22.35 | 13.28 | 5.58 | 3 |
| 80 | 3786 | 13.2 | 22.6 | 5.29 | 1.05 | 41.6 | 93.24 | 35.00 | 22.35 | 13.28 | 5.58 | 3 |
| 81 | 2862 | 10.6 | 20.3 | 5.42 | 0.99 | 47.7 | 92.15 | 32.43 | 23.35 | 13.49 | 5.37 | 3 |
| 82 | 2913 | 10.5 | 19.5 | 5.42 | 0.99 | 46.0 | 92.15 | 32.43 | 23.35 | 13.49 | 5.37 | 3 |
| 83 | 2809 | 10.8 | 19.3 | 5.42 | 0.99 | 44.0 | 92.15 | 32.43 | 23.35 | 13.49 | 5.37 | 3 |
| 84 | 2896 | 10.7 | 19.7 | 5.42 | 0.99 | 45.7 | 92.15 | 32.43 | 23.35 | 13.49 | 5.37 | 3 |
| 85 | 3935 | 15.2 | 23.9 | 5.15 | 1.14 | 36.5 | 94.00 | 33.92 | 22.00 | 15.71 | 5.89 | 3 |
| 86 | 4145 | 14.8 | 23.2 | 5.15 | 1.14 | 36.3 | 94.00 | 33.92 | 22.00 | 15.71 | 5.89 | 3 |
| 87 | 4197 | 14.3 | 22.9 | 5.15 | 1.14 | 37.7 | 94.00 | 33.92 | 22.00 | 15.71 | 5.89 | 3 |
| 88 | 4036 | 15.0 | 23.5 | 5.15 | 1.14 | 36.3 | 94.00 | 33.92 | 22.00 | 15.71 | 5.89 | 3 |
| 89 | 3309 | 12.0 | 20.5 | 5.35 | 0.98 | 41.8 | 93.93 | 35.77 | 23.00 | 16.21 | 5.24 | 3 |
| 90 | 3296 | 12.1 | 21.2 | 5.35 | 0.98 | 42.7 | 93.93 | 35.77 | 23.00 | 16.21 | 5.24 | 3 |
| 91 | 2853 | 11.1 | 19.9 | 5.40 | 1.05 | 44.1 | 91.23 | 34.53 | 23.67 | 16.29 | 5.68 | 3 |
| 92 | 2865 | 11.0 | 19.9 | 5.40 | 1.05 | 44.8 | 91.23 | 34.53 | 23.67 | 16.29 | 5.68 | 3 |